MICROGENOMICS IN AMELOBLASTOMA

Patricia DeVilliers

A thesis submitted to the faculty of the University of North Carolina at Chapel Hill in partial fulfillment of the requirements for the degree of Master of Science in the Department of Dentistry.

Chapel Hill

2006

Approved by

Advisor: Dr. Tim Wright

Reader: Dr. Valerie Murrah

Reader: Dr. Bernard Weissman

ABSTRACT

PATRICIA DEVILLIERS: Microgenomics in Ameloblastoma

(Under the direction of Dr. Tim Wright)

Ameloblastoma, the second most common tumor arising from odontogenic epithelium of the jawbones, is characterized by a benign but locally invasive behavior with a high risk of recurrence. RNA was isolated and amplified from laser capture microdissected (AutoPix™) epithelial cells from five samples of formalin fixed decalcified paraffin embedded, (FFDPE) ameloblastoma tissue. The aminoallyl antisense RNA (aa-aRNA) was hybridized to 40,000-oligonucleotide expression microarrays and compared with Human Universal Reference RNA.

Of the 210 significantly over-expressed genes, many were previously associated with tumor development, including *Ras, cMic, Fos*, *WNT10A*, *FGF13* and T-cell acute lymphocytic leukemia 1. Other genes associated with tumor progression were also noted including Integrins, *IL-17* , *Spondin 2 and* Beta adrenergic receptor kinase 2. Finally polymerase (DNA directed) *gamma 2* , a DNA-repair gene product, was also up-regulated in ameloblastoma.

ACKNOWLEDGEMENTS

To my parents Alfonso and Anita and to my dearest siblings Stella, Federico and Luisé.

To my "Corazón" Adriaan and to my wonderful kids Alex and André, who were very supportive with my ameloblastoma endeavors over the past three years.

To Dr. Tim Wright and Dr. Valerie Murrah for their support and enthusiasm.

TABLE OF CONTENTS

LIST OF TABLES

LIST OF FIGURES

INTRODUCTION

AMELOBLASTOMA

Epidemiology

Tumors arising from epithelium of the odontogenic apparatus or from its derivatives or remnants exhibit considerable histological variation. The World Health Organization classifies the odontogenic tumors into several benign and malignant entities as well as subtypes according to the presence or absence of odontogenic epithelium and odontogenic ectomesenchyme (Barnes et al., 2005). Ameloblastoma is the second most frequently encountered tumor arising from odontogenic epithelium of the jawbones, characterized by a benign but locally invasive behavior with a high risk of recurrence.

In 1995 a review evaluated of the biological profile of 3,677 cases of ameloblastoma from 1,500 journal articles including publications from 1960 to 1993 in English, German, French, Italian, Portuguese, Korean and Japanese (Reichart, Philipsen, & Sonner, 1995). The findings were compared with reviews published by Waldron (Waldron, 1966), (Waldron & el-Mofty, 1987a). The median age in ameloblastoma is 35 years, with a range of 4-92 years. The tumor occurs mainly in younger patients in developing countries. Men and women are equally affected (47%

females and 53% males). While cases have been reported from almost all parts of the world, a higher number of cases occur in Japan, Nigeria and U.S.A. and fewer cases in Australia and South America. Ameloblastomas represent 6%-25% of oral tumors and the percentage in oral biopsies corresponds to 0.04% in Caucasian Americans, 0.3% in African Americans, 5.2% in Nigerians and 6.7% in Asians. In general, it represents only 0.02% - 0.7% of pathology biopsies.

Clinical Features

The main clinical symptoms are painless swelling, delayed tooth eruption, ulceration, mobility and displacement of teeth. The ratio of ameloblastoma of the mandible to maxilla is 5 to 1. About 14% of cases develop in the maxillary sinus and 5% in the nasal cavity. Ameloblastomas arise most frequently in the molar and ascending ramus areas of the mandible except in Africans, where it develops in the anterior region of the jaws. The mandibular tumors occur 12 years earlier than those of the maxilla, having an average size of 4.3 cm. In patients from developing countries, the mandibular tumors have an average size of 6.3 cm compared to those from industrialized countries with 4.2 cm. This may be explained by the difference in access to health care.

Radiographic features

There is an equal number of ameloblastomas that present either as multilocular radiolucent lesions with sharp cortication or as unilocular radiolucencies. Other frequent findings include the presence of an impacted tooth (mostly third molars), root resorption and undefined borderline. Bone cupping can be evident in peripheral ameloblastomas while faint radiopacities are apparent in the desmoplastic variant.

Etiology

Ameloblastoma is thought to originate from sources that include residual tooth germ epithelium, epithelium of odontogenic cysts, stratified squamous epithelium and epithelium of the enamel organ (Vickers & Gorlin, 1970). Several authors describe possible pathogenic mechanisms (Dunsche, Babendererde, Luttges, & Springer, 2003; Mosqueda-Taylor et al., 1997; Reichart et al., 1995) that include nonspecific irritants such as extraction, caries, trauma, infection, inflammation, or tooth eruption, nutritional deficit disorders and viral pathogenesis. No evidence of HPV infection has been detected by morphological examination, immunohistochemistry, in situ hybridization and conventional polymerase chain reaction (Migaldi et al., 2005).

Ameloblastomas according to the WHO classification

The World Health Organization classification of ameloblastomas includes four types: unicystic, solid/multicystic, extraosseous/peripheral and desmoplastic (Barnes et al., 2005). Unicystic ameloblastoma was first described in 1977 by Robinson and Martinez (Robinson & Martinez, 1977). The radiographic appearance of unicystic ameloblastoma is that of a unilocular radiolucency. Cont*Rast*-enhanced MRI (CE-MRI) is useful in differentiating this lesion from keratinizing cystic odontogenic tumor and dentigerous cyst by the observation of low signal intensity on T1-weighted images, high signal intensity on T2-weighted images and relatively thick rim enhancement with/without small intraluminal nodules (Konouchi et al., 2006). Clinically, unicystic ameloblastoma occurs in young patients, before the 5th decade of life (average age of 26 years) (Li, Wu, Yu, & Yu, 2000) and may behave less

aggressively than multilocular lesions, especially if associated with an impacted tooth. Lesions may be treated conservatively (enucleation, curettage), whenever all areas of the cystic lumen are controllable intraoperatively, since it shows lower recurrence rates than multicystic ameloblastomas.

Conventional ameloblastoma (solid/multicystic type) occurs in the jaws, rarely involves the sinonasal cavities and shows a marked preference for the posterior region of the mandible; however, this tumor has a site predilection for the symphysis in African children (Reichart et al., 1995). Most patients present with a multilocular radiolucent lesion; while a higher proportion of multilocular lesions have root resorption when compared with unilocular lesions, there is a higher proportion of unilocular lesions containing an embedded tooth (Fregnani, Fillipi, Oliveira, Vargas, & Almeida, 2002). MRI features show low signal intensity on T1-weighted images, high signal intensity with/without multifocal and markedly high signal intensity corresponding to numerous small cysts on T2-weighted images, and have good enhancement on cont*Rast*-enhanced T1-weighted images (Konouchi et al., 2006). The histologic evaluation of these tumors is based on the cytologic criteria produced by Vickers and Gorlin (Vickers & Gorlin, 1970). Histologically, there are two basic patterns, follicular and plexiform, which carry no clinical relevance. (Barnes et al., 2005). The treatment of choice is radical surgical resection, including bone and adjacent structures, and is indicated to avoid recurrence, particularly when the tumor has eroded the cortical plate and reached the soft tissues. Recurrence can be noted up to ten years after initial treatment, with most cases presenting within the first 5 years (Keszler, Paparella, & Dominguez, 1996; Reichart et al., 1995). Recurrences

in grafts have been reported and may come from the proximal stump, from the adjacent soft tissues, or from intraoperative contamination (Martins & Favaro, 2004).

Desmo**plastic ameloblastoma** is most commonly found in the maxilla, in the anterior/premolar area of the jaws and does not show the typical radiographic features of ameloblastoma. Scattered radiopacities are observed within the radiolucent lesion and can be mistaken for a non-ameloblastomatous lesion or even osteosarcoma (Durmus, Kalayci, Ozturk, & Gunhan, 2003). Histologically, it has pronounced desmoplastic stroma with compressed tumor islands usually lacking a central zone of stellate reticulum (Waldron & el-Mofty, 1987b). Tumor islands often infiltrate into marrow spaces of surrounding bone and there is no capsule formation; recurrence is common but not higher than the other tumor types.

Peripheral ameloblastoma is found exclusively in the gingiva. Theories regarding the origin include development from the extraosseous epithelial remnants of dental lamina and its organ derivatives within the underlying connective tissue. It can also arise from the basal cell layer of the oral mucosa, which is believed to have odontogenic potential (Gurol & Burkes, 1995). Histologically, the peripheral ameloblastoma resembles the intraosseous form. Clinically it presents as a slow growing, asymptomatic sessile, broad, or pedunculated 1- to 2-cm lesion covered by normal mucosa, with a firm consistency, smooth surface, and pink color. Superficial bone resorption is occasionally associated with the lesion. The recommended treatment is wide excision down to the periosteum. Recurrence occurs infrequently (Gavalda, 2005).

Malignant ameloblastoma has recently been sub-classified into metastasizing ameloblastoma and ameloblastic carcinoma on the basis of metastatic spread and cytologic malignant features (Barnes et al., 2005). Ameloblastic carcinoma refers to any ameloblastoma having histological evidence of malignancy in the primary tumor or the recurrent tumor, regardless of whether it has metastasized (Verneuil, Sapp, Huang, & Abemayor, 2002). The term malignant ameloblastoma is reserved for those metastasizing tumors that retain the typical morphology of ameloblastoma, are locally aggressive and have a high recurrence rate of 50–72%. The lungs are the most frequent site of metastases, followed by regional lymph nodes, pleura, vertebrae, skull, diaphragm, liver and the parotid glands. There is one report of bilateral renal metastasis in a patient, where the metastatic lesions showed histologically malignant transformation, even though all primary lesions had benign features (Hayakawa et al., 2004). Genetically, aneuploidy is more common in ameloblastic carcinomas than ameloblastomas and may be predictive of the malignant potential (Muller, DeRose, & Cohen, 1993).

Genetics in Ameloblastoma

Immunoprofiling of ameloblastoma has been the topic of numerous papers in the past years. Expression of cytochrome c, APAF-1, caspase-9, and AIF in tooth germs and ameloblastomas suggests that the mitochondria-mediated apoptotic pathway has a role in apoptotic cell death of normal and neoplastic odontogenic epithelium. Expression of these mitochondrial apoptosis signaling molecules could be involved in oncogenesis, cytodifferentiation, and malignant transformation of odontogenic epithelium (Kumamoto & Ooya, 2005).   There   is   a   relatively   high

frequency of allelic loss in ameloblastic tumors. In order to identify mutational damage in tumor suppressor genes in microdissected samples of ameloblastomas and ameloblastic carcinomas, a panel of polymorphic microsatellite fluorescent-labeled markers/primers was used for multiple suppressor genes on chromosomes 1p, 3p, 9p,10q, and 17p (L-myc, hOGG1, p16, pten, and p53). Analysis of the tumor PCR products showed the highest frequency of loss at L-myc and pten. The frequencies varied somewhat between different tumor types but were not significantly different between the carcinomas and the benign tumors. Therefore, testing for allelic loss is not expected to provide clinical prognostic information (Nodit et al., 2004).

Chromosomal imbalances in ameloblastomas appear to be rare with losses in chromosomes 22 and 10 being the most frequently described (Jaaskelainen et al., 2002). Deregulation of several genes in normal tooth development could play a role in the histogenesis of ameloblastoma. The cloning and characterization of expression of the ameloblastin (*AMBN*) and amelogenin genes in these tumors supports the hypothesis that ameloblastomas arise from the dental lamina, the outer enamel epithelium or the inner enamel epithelium (Kumamoto, Yoshida, & Ooya, 2001). The undifferentiated phenotype of neoplastic cells could result from a direct action of *AMBN* in the target tissue or an indirect effect due to reciprocal signaling between the epithelial and mesenchymal components (Perdigao, Gomez, Pimenta, & De Marco, 2004).

Gene expression alterations were identified for the first time in six odontogenic tumors by the use of cDNA microarrays containing 19,000 human cDNAs. (Carinci et

al., 2003). Statistical analysis identified 506 genes associated with the tumors. 43 cDNAs differentiated the three malignant odontogenic tumors (ameloblastic carcinoma, clear cell odontogenic tumor and granular cell odontogenic tumor) from the three benign ameloblastoma biopsies.

Gene expression profiling of ameloblastomas, using a commercial cDNA microarray with 588 cancer-related human cDNA fragments, has also been performed by using tooth germs as the reference tissue. Previous investigators showed that 34 genes had different levels of expression in the tumors compared with the tooth germs. *FOS* was the most highly over-expressed and 7 other genes such as Sonic Hedge Hog *SHH* and genes related to cell adhesion were under-expressed in all tumors (Heikinheimo et al., 2002). Consequently, the possible role of *SHH* signaling molecules (*SHH*, *PTC*, SMO, *GLI1*) was studied in benign and malignant ameloblastoma, using RT-PCR and standard immunohistochemistry (IHC) with antibodies for the different *SHH* molecules. Results showed that mRNA transcripts were expressed in all the tumors and tooth germs, with no difference between benign and malignant tumors. Similar results were seen with the IHC levels where reactivity was found for all the *SHH* antibodies at somewhat variable degrees in different tissues. Therefore, *SHH* signal transduction seems to have a specific role in oncogenesis of odontogenic epithelium (Zhang et al., 2005).

Many other immunohistochemical studies have been reported in the literature as an attempt to understand the mechanism of development of ameloblastomas. Differences in p53 protein expression in different types of ameloblastomas have implicated tumor suppressor gene alteration as a potential oncogenic mechanism

(Toida et al., 2005). Apoptotic cell death in ameloblastomas (especially granular cell type) is increased, suggesting that apoptosis pathways also may be involved in tumorigenesis (Kumamoto & Ooya, 2005; Sandra, Hendarmin, Nakao, Nakamura, & Nakamura, 2005). Parathyroid hormone-related protein (*PTHrP*) has been demonstrated in ameloblastoma and could play a significant role in local bone resorption, offering at least partial explanation for the tumor's infiltrative growth and destructive behavior. The uniformity of *PTHrP* expression may have therapeutic implications, particularly through PTHrP-blocking treatment modalities (Abdelsayed, Vartanian, Smith, & Ibrahim, 2004).

MICROGENOMICS

Since the sequencing of the human genome was completed, microgenomics is a powerful experimental approach, employing highly sophisticated, high-throughput platforms. However, these mainly chip-based methodologies can only generate biologically relevant data if the samples consist of homogenous cell populations, in which no unwanted cells of different specificity and/or developmental stage obscure the results.

Different methods have been routinely applied to overcome the problem presented by heterogeneous samples, e.g., global surveys, cell cultures and microdissection. Recently, laser-assisted microdissection methods have allowed for fast and precise procurement of extremely small samples. Through subsequent application of methods of linear mRNA amplification in a pool of isolated total RNA, it is now possible to perform high-throughput RNA expression profiling by microdissecting and processing even single-cell samples. Molecular profiling is now

increasingly important to the simultaneous study of many genes or proteins. Among the profiling platforms, the oligonucleotide array is applied to generate specific genetic fingerprints for individual lesions or distinct cell populations (Schena, Shalon, Davis, & Brown, 1995).

Originally, microdissection meant manually scraping off an area of interest from a sectioned tissue by the means of fine needles (Schena et al., 1998). The first laser-assisted microdissection method used selective ultraviolet radiation fractionation followed by polymerase chain reaction (PCR) to analyze specific cell subsets present on a microscope section (Shibata et al., 1992). A non-damaging, precise and fast method of laser-assisted cell selection was developed, the laser capture microdissection (LCM) process, at the National Institutes of Health (NIH) (Emmert-Buck et al., 1996). LCM selects the desired cells and tissue areas from a microscopic slide. The cells of interest are transferred onto a thin thermoplastic ethylene vinyl acetate film by pulsing of an infrared laser. The focally-softened film temporarily expands onto the targeted cell(s) and attaches to them. When the film, which is mounted to a plastic cap, is lifted off the microscopic sample slide, the tissue section shears at the edges of the tissue/polymer compound and the selected cells are removed along with the film and cap. Very small and highly complex structures can be easily microdissected by this method, including single cells (Luo et al., 1999).

Laser capture microdissection (LCM) can be used for molecular downstream analysis because the nucleic acids as well as the proteins are maintained intact and unaltered by the sampling process, as it does not generate any chemical bonds to

10

the dissected cells (Webb, 2000). Furthermore, the RNA does not suffer any LCM-derived impacts on quality, making it possible to use LCM to catalog the gene expression profiles of normal, precancerous, and malignant cells (Leethanakul et al., 2000; Ohyama et al., 2000).

Laser-assisted microdissection is a fast way of precisely obtaining small samples or even single-cell samples, but the total RNA in such samples is usually too small for gene expression assays to be conducted. Expression profiling platforms typically require microgram quantities of RNA to be hybridized onto the arrays (Ohyama et al., 2002)(39). Luo et al. were the first to use LCM along with linear amplification of the isolated RNA (Luo et al., 1999). These two techniques together make it possible to generate, compare, and cont*Ras*t gene expression profiles using only a small number of cells per sample. Numerous studies have been published, procuring small and homogenous samples, isolating the total RNA and amplifying its mRNA portion by linear T7-based protocols (Alevizos et al., 2001; Mohr et al., 2004; Naderi et al., 2004; Wu et al., 2005). This amplification method is now commonly known as the Eberwine protocol (Van Gelder et al., 1990). In a two-step process, double-stranded cDNA is generated from mRNA while, simultaneously, a T7 promoter sequence is introduced. T7 polymerase   is subsequently used to synthesize antisense-oriented RNA (aRNA) off this cDNA template, thereby amplifying the original template amounts up to 80-fold (Luo et al., 1999; Ohyama et al., 2000; Ohyama et al., 2002). Currently, it is possible to amplify the original mRNA pool of a given sample up to 1,000,000-fold or even 10,000,000-fold through two rounds of subsequent linear amplifications, without introducing bias

into the samples. This allows working with as little as 10 intact cells or 50 microdissected sectioned cells and still being able to generate enough aRNA for downstream array analysis.

(Coco et al., 2005; King et al., 2005; Mohr et al., 2004; Naderi et al., 2004).

Studies using the tools and methods of microgenomics have shed light on how those new approaches will eventually aid in the development of a new generation of diagnostics, e.g., leading to new patient-specific drugs tailored to the requirements assessed by assaying only a few biopsy cells (Taylor et al., 2004). In the present study we apply microgenomics to evaluate the gene expression profile of ameloblastomas. The goal of this study is to gain an understanding of the molecular mechanisms involved in initiating and maintaining tumorigenesis of this odontogenic tumor.

REFERENCES

Abdelsayed, R. A., Vartanian, R. K., Smith, K. K., & Ibrahim, N. A. (2004). Parathyroid hormone-related protein (PTHrP) expression in ameloblastoma. *Oral Surgery, Oral Medicine, Oral Pathology, Oral Radiology, and Endodontics, 97*(2), 208-219.

Alevizos, I., Mahadevappa, M., Zhang, X., Ohyama, H., Kohno, Y., & Posner, M. et al. (2001). Oral cancer in vivo gene expression profiling assisted by laser capture microdissection and microarray analysis. *Oncogene, 20*(43), 6196-6204.

Barnes, L., Eveson, J. W., Reichart, P., & Sidransky, D. (2005). *Pathology and genetics of head and neck tumors* (IARC WHO Classification of Tumours, No 9 ed.). Switzerland: WHO Press.

Carinci F, Francioso F, Piattelli A, Rubini C, Fioroni M, Evangelisti R, Arcelli D, Tosi L, Pezzetti F, Carinci P, Volinia S. (2003). Genetic expression profiling of six odontogenic tumors. J. Dent. Research 2003 Jul;82(7):551-7.

Coco, S., Defferrari, R., Scaruffi, P., Cavazzana, A., Di Cristofano, C., & Longo, L. et al. (2005). Genome analysis and gene expression profiling of neuroblastoma and ganglioneuroblastoma reveal differences between neuroblastic and schwannian stromal cells. *The Journal of Pathology, 207*(3), 346-357.

Dunsche, A., Babendererde, O., Luttges, J., & Springer, I. N. (2003). Dentigerous cyst versus unicystic ameloblastoma--differential diagnosis in routine histology. *Journal of Oral Pathology & Medicine : Official Publication of the International Association of Oral Pathologists and the American Academy of Oral Pathology, 32*(8), 486-491.

Durmus, E., Kalayci, A., Ozturk, A., & Gunhan, O. (2003). DeSMOplastic ameloblastoma in the mandible. *The Journal of Craniofacial Surgery, 14*(6), 873-875.

Emmert-Buck, M. R., Bonner, R. F., Smith, P. D., Chuaqui, R. F., Zhuang, Z., & Goldstein, S. R. et al. (1996). Laser capture microdissection. *Science, 274*(5289), 998-1001.

Fregnani, E. R., Fillipi, R. Z., Oliveira, C. R., Vargas, P. A., & Almeida, O. P. (2002). Odontomas and ameloblastomas: Variable prevalences around the world? *Oral Oncology, 38*(8), 807-808.

Gavalda, C. (2005). Peripheral ameloblastoma. *Med.Oral Patol.Oral Cir.Bucal, 10*(2), 187.

Gurol, M., & Burkes, E. J.,Jr. (1995). Peripheral ameloblastoma. *Journal of Periodontology, 66*(12), 1065-1068.

Hayakawa, K., Hayashi, E., Aoyagi, T., Hata, M., Kuramoto, C., & Tonogi, M. et al. (2004). Metastatic malignant ameloblastoma of the kidneys. *International Journal of Urology : Official Journal of the Japanese Urological Association, 11*(6), 424-426.

Heikinheimo, K., Jee, K. J., Niini, T., Aalto, Y., Happonen, R. P., & Leivo, I. et al. (2002). Gene expression profiling of ameloblastoma and human tooth germ by means of a cDNA microarray. *Journal of Dental Research, 81*(8), 525-530.

Jaaskelainen, K., Jee, K. J., Leivo, I., Saloniemi, I., Knuutila, S., & Heikinheimo, K. (2002). Cell proliferation and chromosomal changes in human ameloblastoma. *Cancer Genetics and Cytogenetics, 136*(1), 31-37.

Keszler, A., Paparella, M. L., & Dominguez, F. V. (1996). Desmoplastic and non-deSMOplastic ameloblastoma: A comparative clinicopathological analysis. *Oral Diseases, 2*(3), 228-231.

King, C., Guo, N., Frampton, G. M., Gerry, N. P., Lenburg, M. E., & Rosenberg, C. L. (2005). Reliability and reproducibility of gene expression measurements using amplified RNA from laser-microdissected primary breast tissue with oligonucleotide arrays. *Journal of Molecular Diagnostics : JMD, 7*(1), 57-64.

Konouchi, H., Asaumi, J. I., Yanagi, Y., Hisatomi, M., Kawai, N., & Matsuzaki, H. et al. (2006). Usefulness of cont*Rast* enhanced-MRI in the diagnosis of unicystic ameloblastoma. *Oral Oncology,*

Kumamoto, H., & Ooya, K. (2005). Expression of tumor necrosis factor alpha, TNF-related apoptosis-inducing ligand, and their associated molecules in ameloblastomas. *Journal of Oral Pathology & Medicine : Official Publication of the International Association of Oral Pathologists and the American Academy of Oral Pathology, 34*(5), 287-294.

Kumamoto, H., Yoshida, M., & Ooya, K. (2001). Immunohistochemical detection of amelogenin and cytokeratin 19 in epithelial odontogenic tumors. *Oral Diseases, 7*(3), 171-176.

Leethanakul, C., Patel, V., Gillespie, J., Shillitoe, E., Kellman, R. M., & Ensley, J. F. et al. (2000). Gene expression profiles in squamous cell carcinomas of the oral cavity: Use of laser capture microdissection for the construction and analysis of stage-specific cDNA libraries. *Oral Oncology, 36*(5), 474-483.

Li, T. J., Wu, Y. T., Yu, S. F., & Yu, G. Y. (2000). Unicystic ameloblastoma: A clinicopathologic study of 33 chinese patients. *The American Journal of Surgical Pathology, 24*(10), 1385-1392.

Luo, L., Salunga, R. C., Guo, H., Bittner, A., Joy, K. C., & Galindo, J. E. et al. (1999). Gene expression profiles of laser-captured adjacent neuronal subtypes. *Nature Medicine, 5*(1), 117-122.

Martins, W. D., & Favaro, D. M. (2004). Recurrence of an ameloblastoma in an autogenous iliac bone graft. *Oral Surgery, Oral Medicine, Oral Pathology, Oral Radiology, and Endodontics, 98*(6), 657-659.

Migaldi, M., Pecorari, M., Rossi, G., Maiorana, A., Bettelli, S., & Tamassia, M. G. et al. (2005). Does HPV play a role in the etiopathogenesis of ameloblastoma? an immunohistochemical, in situ hybridization and polymerase chain reaction study of 18 cases using laser capture microdissection. *Modern Pathology : An Official*

Journal of the United States and Canadian Academy of Pathology, Inc, 18(2), 283-289.

Mohr, S., Bottin, M. C., Lannes, B., Neuville, A., Bellocq, J. P., & Keith, G. et al. (2004). Microdissection, mRNA amplification and microarray: A study of pleural mesothelial and malignant mesothelioma cells. *Biochimie, 86*(1), 13-19.

Mosqueda-Taylor, A., Ledesma-Montes, C., Caballero-Sandoval, S., Portilla-Robertson, J., Ruiz-Godoy Rivera, L. M., & Meneses-Garcia, A. (1997). Odontogenic tumors in mexico: A collaborative retrospective study of 349 cases. *Oral Surgery, Oral Medicine, Oral Pathology, Oral Radiology, and Endodontics, 84*(6), 672-675.

Muller, S., DeRose, P. B., & Cohen, C. (1993). DNA ploidy of ameloblastoma and ameloblastic carcinoma of the jaws. analysis by image and flow cytometry. *Archives of Pathology & Laboratory Medicine, 117*(11), 1126-1131.

Naderi, A., Ahmed, A. A., Barbosa-Morais, N. L., Aparicio, S., Brenton, J. D., & Caldas, C. (2004). Expression microarray reproducibility is improved by optimising purification steps in RNA amplification and labelling. *BMC Genomics [Computer File], 5*(1), 9.

Nodit, L., Barnes, L., Childers, E., Finkelstein, S., Swalsky, P., & Hunt, J. (2004). Allelic loss of tumor suppressor genes in ameloblastic tumors. *Modern Pathology : An Official Journal of the United States and Canadian Academy of Pathology, Inc, 17*(9), 1062-1067.

Ohyama, H., Mahadevappa, M., Luukkaa, H., Todd, R., Warrington, J. A., & Wong, D. T. (2002). Use of laser capture microdissection-generated targets for hybridization of high-density oligonucleotide arrays. *Methods in Enzymology, 356*, 323-333.

Ohyama, H., Zhang, X., Kohno, Y., Alevizos, I., Posner, M., & Wong, D. T. et al. (2000). Laser capture microdissection-generated target sample for high-density oligonucleotide array hybridization. *BioTechniques, 29*(3), 530-536.

Perdigao, P. F., Gomez, R. S., Pimenta, F. J., & De Marco, L. (2004). Ameloblastin gene (AMBN) mutations associated with epithelial odontogenic tumors. *Oral Oncology, 40*(8), 841-846.

Reichart, P. A., Philipsen, H. P., & Sonner, S. (1995). Ameloblastoma: Biological profile of 3677 cases. *European Journal of Cancer. Part B, Oral Oncology, 31B*(2), 86-99.

Robinson, L., & Martinez, M. G. (1977). Unicystic ameloblastoma: A prognostically distinct entity. *Cancer, 40*(5), 2278-2285.

Sandros J, Heikinheimo K, Happonen RP, Stenman G., (1991) Expression of p21RAS in odontogenic tumors. *APMIS* Jan;99(1):15-20

Sandra, F., Hendarmin, L., Nakao, Y., Nakamura, N., & Nakamura, S. (2005). Inhibition of akt and MAPK pathways elevated potential of TNFalpha in inducing apoptosis in ameloblastoma. *Oral Oncology*

Schena, M., Heller, R. A., Theriault, T. P., Konrad, K., Lachenmeier, E., & Davis, R. W. (1998). Microarrays: Biotechnology's discovery platform for functional genomics. *Trends in Biotechnology, 16*(7), 301-306.

Schena, M., Shalon, D., Davis, R. W., & Brown, P. O. (1995). Quantitative monitoring of gene expression patterns with a complementary DNA microarray. *Science, 270*(5235), 467-470.

Shibata, D., Hawes, D., Li, Z. H., Hernandez, A. M., Spruck, C. H., & Nichols, P. W. (1992). Specific genetic analysis of microscopic tissue after selective ultraviolet radiation fractionation and the polymerase chain reaction. *American Journal of Pathology, 141*(3), 539-543.

Taylor, T. B., Nambiar, P. R., Raja, R., Cheung, E., Rosenberg, D. W., & Anderegg, B. (2004). Microgenomics: Identification of new expression profiles via small and single-cell sample analyses. *Cytometry A., 59*(2), 254-261.

Toida, M., Balazs, M., Treszl, A., Rakosy, Z., Kato, K., & Yamazaki, Y. et al. (2005). Analysis of ameloblastomas by comparative genomic hybridization and fluorescence in situ hybridization. *Cancer Genetics and Cytogenetics, 159*(2), 99-104.

Van Gelder, R. N., von Zastrow, M. E., Yool, A., Dement, W. C., Barchas, J. D., & Eberwine, J. H. (1990). Amplified RNA synthesized from limited quantities of heterogeneous cDNA. *Proceedings of the National Academy of Sciences of the United States of America, 87*(5), 1663-1667.

Verneuil, A., Sapp, P., Huang, C., & Abemayor, E. (2002). Malignant ameloblastoma: Classification, diagnostic, and therapeutic challenges. *American Journal of Otolaryngology, 23*(1), 44-48.

Vickers, R. A., & Gorlin, R. J. (1970). Ameloblastoma: Delineation of early histopathologic features of neoplasia. *Cancer, 26*(3), 699-710.

Waldron, C. A. (1966). Ameloblastoma in perspective. *Journal of Oral Surgery (American Dental Association : 1965), 24*(4), 331-333.

Waldron, C. A., & el-Mofty, S. K. (1987a). A histopathologic study of 116 ameloblastomas with special reference to the deSMOplastic variant. *Oral Surgery, Oral Medicine, and Oral Pathology, 63*(4), 441-451.

Waldron, C. A., & el-Mofty, S. K. (1987b). A histopathologic study of 116 ameloblastomas with special reference to the deSMOplastic variant. *Oral Surgery, Oral Medicine, and Oral Pathology, 63*(4), 441-451.

Webb, T. (2000). Laser capture microdissection comes into mainstream use. *Journal of the National Cancer Institute, 92*(21), 1710-1711.

Wu, M. S., Lin, Y. S., Chang, Y. T., Shun, C. T., Lin, M. T., & Lin, J. T. (2005). Gene expression profiling of gastric cancer by microarray combined with laser capture microdissection. *World J.Gastroenterol., 11*(47), 7405-7412.

Zhang, L., Chen, X. M., Sun, Z. J., Bian, Z., Fan, M. W., & Chen, Z. (2005). Epithelial expression of *SHH* signaling pathway in odontogenic tumors. *Oral Oncology*

MICROGENOMICS IN AMELOBLASTOMA

Background: Ameloblastoma, the second most common tumor arising from odontogenic epithelium of the jawbones, is characterized by a benign, but locally invasive, behavior with a high risk of recurrence. Microgenomics employs highly sophisticated, high-throughput platforms that can generate biologically relevant data if the samples investigated consist of homogenous cell populations. The purpose of this study was to carry out and analyze the gene expression profile of ameloblastoma using microgenomics.

Methods: RNA was isolated from epithelial cells and amplified from five samples of formalin fixed decalcified paraffin embedded, (FFDPE) plexiform ameloblastoma tissue using laser capture microdissection (AutoPix™). The aminoallyl antisense RNA (aa-aRNA) was hybridized to 40,000-oligonucleotide expression microarrays and compared with Human Universal Reference RNA.

Results: Of the 210 significantly over-expressed genes, many were previously associated with tumor development, including *Ras, cMic, Fos*, *WNT10A*, *FGF13* and T-cell acute lymphocytic leukemia 1. Other genes associated with tumor progression were also noted including Integrins, *IL-17, Spondin 2 and* Beta, adrenergic, receptor kinase 2. Finally polymerase (DNA directed), *gamma 2,* a DNA-repair gene product, was also up-regulated in ameloblastoma. Studies using the tools and methods of

microgenomics of assessing only a few biopsy cells, combined with the analysis of tumorigenesis pathways will eventually aid in the development of a new generation of diagnostics and therapeutic tools in the management of ameloblastoma.

Key terms: microgenomics; laser capture microdissection; ameloblastoma.

INTRODUCTION

Ameloblastoma is the second most frequently encountered tumor arising from odontogenic epithelium of the jawbones and is characterized by a benign but locally invasive behavior with a high risk of recurrence. Ameloblastomas are classified as solid/multicystic type, extraosseous/peripheral type, desmoplastic type and unicystic type (Barnes et al., 2005). Gene expression profiles were characterized for the first time in six odontogenic tumors using cDNA microarrays containing 19,000 human cDNAs. (Carinci et al., 2003). Statistical analysis identified 506 differentially expressed genes that were associated with the tumors. 43 cDNAs differentiated the three malignant odontogenic tumors (ameloblastic carcinoma, clear cell odontogenic tumor and granular cell odontogenic tumor) from the three benign ameloblastoma biopsies. Another gene expression profiling of ameloblastomas, using a commercial cDNA microarray target with 588 cancer-related human cDNA fragments, was performed by examining frozen tooth germs and ameloblastomas. A total of 34 genes expressed levels in the tumors that were different from the tooth germs. *FOS* was the most highly over-expressed and 7 other genes such as *SHH* and genes related to cell adhesion were under-expressed in all tumors (Heikinheimo et al., 2002). Consequently, a possible role of *SHH* signaling molecules (*SHH*, *PTC*, *SMO*,

GLI1) was investigated in benign and malignant ameloblastoma suggesting that the expression of SHH, PTC and SMO, might play a role in epithelial-mesenchymal interactions and cell proliferation not only in normal tooth development as well as in tumorigenesis of ameloblastoma (Kumamoto,H. 2004; Zhang,L. 2005).

A major challenge that precludes the genetic analysis of tumor tissue has been the technical difficulty of collecting pure populations of specific cells directly from complex heterogeneous tissue. Laser capture microdissection (LCM) is a technique that allows the isolation of individual cell populations for genetic analysis, thereby circumventing the impact of tissue heterogeneity. (Emmert-Buck et al., 1996; Webb, 2000). Laser Capture microdissection (LCM) has proven to be an effective tool to isolate single cells with no detrimental effect on PCR amplification of DNA or RNA. LCM can be easily coupled with high density oligonucleotide array technology to obtain expression profiles from discrete cell populations in histologically complex tumors. Qualitative and quantitative assessment of isolated cellular RNA and inclusion of a set of internal transcript controls to monitor assay fidelity can greatly contribute to the success of this approach (Luzzi, Holtschlag, & Watson, 2001; Luzzi, Mahadevappa, Raja, Warrington, & Watson, 2003).

The purpose of this study was to carry out and analyze the gene expression profile of the ameloblastoma basal cell layer using microgenomics with highly sophisticated, high-throughput platforms that can generate biologically relevant data if the samples investigated consist of homogenous cell populations.

This study is the first to report the results of combining LCM and microarray gene expression profiling in formalin fixed decalcified paraffin embedded

ameloblastoma cells. Our results showed overexpression of *Ras, cMic, Fos*, *WNT10A*, *FGF13* and T-cell acute lymphocytic leukemia 1. Also, Integrins, *IL-17, Spondin 2 and* Beta adrenergic receptor kinase 2 were noted.

MATERIALS AND METHODS

Ameloblastoma samples

This study was approved by the Institutional Review Board. The tissue samples were obtained from the paraffin block archives of the University of North Carolina Surgical Pathology Department that included the diagnosis of ameloblastoma. Five cases were selected based on the histological diagnosis following the criteria from the 2005 World Health Organization Histological Typing of Odontogenic Tumors.

Formalin fixed paraffin embedded ameloblastoma tissue, dating back to 2004, had been previously decalcified in Richard Allan Scientifics' Decalcifying Solution containing water, hydrochloric acid, ethylenediaminetetraacetic acid, tetra sodium tartrate, potassium sodium and tartrate. This decal solution offers rapid decalcification without destroying nuclear properties of the tissue. Glass slides for laser microdissection and microgenomics analysis were prepared from the formalin fixed, decalcified, paraffin embedded (FFDPE) tissue blocks following the protocol from ParadigmArrayLabs™ and adapted from Arcturus Paradise Reagent System User Guide. RNase contamination from glass, work surfaces and equipment was removed using RNase*Zap*® Solution. Multiple sections, 7 µm thick, were cut from each sample block. The slides were air-dry for 30 minutes at room temperature. A total of 75 slides (15 from each ameloblastoma block sample) were prepared, RNA was extracted and amplified from the basal cell layer cells obtained by Laser

Capture Microdissection (LCM) using Arcturus' AutoPix™ (Mountain View, CA), followed by labeling and hybridization of aa-aRNA for generation of gene expression profile. These steps were carried out by ParadigmArrayLabs™.

Reverse Transcription - quantitative Polymerase **Chain Reaction (RT-qPCR) from tissue scrapes**: To test the fidelity of the RNA, five slides (one for each ameloblastoma sample) were stained with hematoxylin-eosin follow by tissue scraping and RNA extraction following the protocol of Optimum™ FFPE RNA Isolation Kit from Ambion, Inc. Austin, TX.   The RNA extracted from the tissue scrape samples was used to make complementary DNA (cDNA) via reverse transcription and Real Time- PCR was used to measure the RNA quality and quantity. In addition to the RNA samples, a control RNA was run to serve as template for a standard curve enabling quantitation of the sample material. Two primer sets were designed for beta-actin mRNA. The assessment protocol for the quality of RNA in FFPE tissue blocks measures the average beta-actin cDNA length by quantification of the PCR product yield from the 3' end primer (primer 1107-1181) and another relative 5' sequence (primer 697-773). The ratio of the RNA quantity 3' and 5' beta-actin Ct (threshold cycle) is an indicator of the quality of amplified RNA. A ratio value up to 10 indicates good RNA quality for microarray analyses and ratio value above 50 represent poorer quality RNA.

Reverse Transcription equivalent score (RTE score): The RT score is a better predictor of the input amount for the RNA amplification reaction than the actual mass of the material. In parallel with the standard curve for the aRNA, the qPCR is performed for the diluted/non-diluted scraped sample. The 3'Ct values versus a

known amount of diluted/non-diluted scraped sample are plotted into a linear type chart. The 3'Ct value for 100pg uRNA, recorded from the standard curve, is plotted in the linear chart of the scrape sample and identifies the corresponding amount of the scrape sample.

Laser capture microdissection (LCM): Once the quantity and quality of total RNA from the tissue scrapes were established, the cells from the basal layer of the ameloblastoma tissue in the five sample slides were cut using the AutoPix™ laser capture microdissection system with an infrared diode laser (Arcturus Engineering, Santa Clara, CA, USA). The AutoPix™ LCM is an automated platform for high-throughput microdissection of individual cells or multi-cellular structures from tissue sections. The process preserves spatial and cellular integrity throughout and enables accurate quality control of the cells selected for downstream analysis. A decision was made to microdissect the cells from the basal cell layer of the ameloblastoma rather than the stellate-like reticulum area to establish a baseline and to avoid the variability that metaplastic changes can confer to the stellate-like reticulum. In order to correctly identify the cells to be microdissected, H&E sections of the samples were scanned using the ScannScope™ system, at a magnification of 40X. The scanned images were then viewed with the Aperio™ software. The tissue slides used for LCM were stained by ParadygmArrayLab™ with Hematoxylin and Eosin Stain. The samples were sealed in a completely enclosed environment during microdissection to minimize environmental effects and sample contamination. Each step of the microdissection process was documented with photographs. During the microdissection procedure, a CapSure™ cap was positioned over the tissue section

and at the end of the LCM the transparent thermoplastic film, which covers the cap, was peeled off and placed into the RNA extraction buffer. Total RNA was extracted from the microdissected cells following the protocol of Optimum™ FFPE RNA Isolation Kit from Ambion, Inc. Austin, TX. Before proceeding to the amplification, total RNA was quantified using the Nanodrop ND-1000 spectrophotometer (NanoDrop Technologies, Inc., Montchanin, DE) and the quality assessed by the 2100 electrophoresis bioanalyzer. (Agilent Technologies, Inc, Palo Alto, CA).

RNA amplification: To generate antisense RNA (aRNA) by amplifying polyadenylated mRNA present in total RNA from the laser-captured samples, the TargetAmp™ 2-Round Aminoallyl-aRNA Amplification Kit from Epicentre® Biotechnologies was used. The protocol uses an improved "Eberwine"(Van Gelder et al., 1990) linear amplification process for amplifying Poly(A) RNA using the RTE score as an input for the total RNA. In parallel with the laser-captured samples, two other samples were included in the amplification: a positive control (human universal RNA) and a negative control (no RNA template). The TargetAmp 2-Round Aminoallyl-aRNA Amplification procedure protocol is briefly described as follows:

1. First-strand cDNA Synthesis: The Poly (A) RNA component of a total RNA sample was reversed transcribed into first strand cDNA. The reaction was primed from a synthetic oligo (dT) primer containing a phage T7 RNA Polymerase promoter sequence at its 5'-end. First strand cDNA synthesis was catalyzed by SuperScript III Reverse Transcriptase and performed at an elevated temperature to reduce RNA secondary structure.

2. Second-strand cDNA Synthesis: The RNA component of the cDNA/RNA hybrid produced in Step 1 was digested into small RNA fragments using an RNase H enzyme and the primed to 2nd strand cDNA. The resulting product was a double-stranded cDNA containing a T7 transcription promoter in an orientation that generated anti-sense RNA (aRNA) during the subsequent *in vitro* transcription reaction. The cDNA produced was used in the *In Vitro* transcription reaction without the need for purification.

3. *In vitro* Transcription of Aminoallyl-aRNA: High yields of aminoallyl-aRNA were produced in a rapid *in vitro* transcription reaction that utilized the double-stranded cDNA produced in Step 2. In the transcription reaction, the canonical UTP nucleotide was partially substituted for with 5-(3-aminoallyl)-UTP aminoallyl-UTP; AA-UTP).

Oligonucleotide Microarray Analysis: This study used the Whole Human Genome Oligo Microarray (G4112A) (Agilent Technologies Inc, Palo Alto, California). 60-mer oligonucleotides (double density format) probe sequences represent over 40,000 human genes and transcripts on a 1"x 3" (25mm x 75mm) glass slide, enabling the whole-genome screening on a single microarray slide. Target labeling, hybridization, washing, scanning, and data extraction were performed following the Oligonucleotide Microarray Hybridization Protocol as previously described for the analysis of Eukaryotic RNA (Ohyama et al., 2000; Ohyama et al., 2002)

In this project, RNA amplified from FFDPE samples was labeled with the Cy5 dye and hybridized to the Agilent™ array with a Cy3-labeled Stratagene Human Universal Reference sample (Novoradovskaya, Whitfield, Basehore, Novoradovsky, Pesich, Usary, Karaca, Wong, Aprelikova, Fero, Perou, Botstein, & Braman, 2004a).

The labeled cRNA from a single labeling reaction was used in all five hybridizations to minimize technical variance.

Data analysis: The stained arrays were scanned at 488 nm using a G2500 Scanner (Agilent, Palo Alto, CA). Statistical analysis of the microarray data was performed using Genespring™ software as well as Significance Analysis of Microarrays (SAM) (Larsson, Wahlestedt, & Timmons, 2005; Tusher, Tibshirani, & Chu, 2001). This statistical method interfaces with Microsoft Excel to determine if the expression of any genes is significantly related to the response variable.

When testing the statistical significance for many genes, different methods of multiple testing corrections can be used to adjust the individual p-value to account for the effect of chance. In this study, we used the Benjamini and Hochberg false discovery rate, which is defined as the proportion of genes expected to occur by chance (assuming genes are independent) relative to the proportion of identified genes. There was no way to calculate this in advance, so the statement about the number expected will simply say that the expected number of genes by chance is 100 % of the genes identified. This procedure provides a good balance between discovery of significant genes and protection against false positives. The occurrence of the latter is held to a small proportion of the list, and is probably a good choice of multiple-testing correction for most situations.

RESULTS

RNA, aRNA, and Array Quality: RNA assessment from tissue scrapes: The amount of total RNA yield from the tissue scrapes had a low 260/280 ratio, between 1.39 and 1.74 (expected range 1.8 – 2.1) due to the degradation of RNA after

formalin fixation of the tissue. Values for the tissue scrape samples are included in the appendix under Table A1 as well as the standard curves for this experiment under Figure A1.

Generation of gene expression profile using LCM: Laser capture microdissection used to isolate pure populations of basal cell layer ameloblastoma cells from formalin fixed decalcified paraffin embedded (FFDPE) samples yielded an estimated 500 cells and approximately 100-500 ng total RNA. The values for the Total RNA characterization are included in the appendix under Table A2.

The antisense RNA (aRNA) of 500 - 1,000 bp in length that was generated by two round amplifications showed a 260/280 ratio within an acceptable range. Anti-sense RNA generated from the ameloblastoma samples had an average size of 500 nucleotides, indicating that good quality RNA was obtained reliably from LCM-captured cells. The correlation between the phenotype of each sample, the histological presentation, the LCM extracted cells as well as the graphic representation of the aRNA is depicted in Table 1. All samples show similar histological pattern; the LCM cell follow the pattern of the basal cell layer, while the curve depicting the quality of the aRNA is consistent in all five samples. The characterization of the amynoallyl-antisense RNA (aa-aRNA) obtained from the samples is presented in Table A3 in the appendix. The yield of aminoallyl aRNA was, in all cases, sufficient to hybridize to the oligonucleotide array, which was performed following protocols previously described. (Luo et al., 1999)(Leethanakul et al., 2003). Oligonucleotide arrays have been reported as particularly attractive for

gene expression studies because they can readily distinguish expression levels of closely related gene family members. (King et al., 2005).

Gene expression profile analysis**:** A normalization factor was estimated from ratios of the medians of the expression profiles. Normalization was performed by adding the log2 of the normalization factor to the log2 of the ratio of the medians. The log2 ratios for all the targets on the array were then calibrated using the normalization factor, and log2 ratios outside the 99.7% confidence interval were determined as significantly changed in the ameloblastoma samples. Scatter plots of the gene intensities of the samples are shown in Table A4 included in the appendix.

Statistical analysis: Genespring® platform provided a comprehensive statistical analysis showing a total of 38 genes that were 2 fold up-regulated, all of which were present in all 5 samples. No down–regulated genes were filtered out at a significant *P* value. (Benjamini and Hochberg false discovery rate filter). This can be attributed to the stringency of the algorithm and to the fact that sample number 1 varied the most in its gene expression profile, when compared with samples 2, 3, 4 and 5. A possible explanation is that sample number 1 represented a case of recurrent ameloblastoma. Further studies would be useful to investigate the difference in genes expression between primary and recurrent ameloblastomas. Hierarchical clustering of the 5 arrays, 2-fold up and down-regulated genes is represented in Figure 1 and shows how samples 4 and 5 shared common gene expression; samples 2 and 3 have similar expression between them, while sample 1 is different to the other four samples and is the closest to the human uRNA reference (It may represent a different gene expression in a recurrent ameloblastoma). Table 2 shows

a partial list of 2-fold upregulated genes including annotations regarding their biological process, molecular function and pathways.

The gene lists were also submitted to the Significance Analysis of Microarrays (SAM) which provides an estimate of False Discovery Rate for multiple testing. Table A5 in the appendix illustrates an example of SAM analysis for a dataset. A total of 10 up-regulated genes and 41 down-regulated genes, 2-fold, were present in all 5 samples. In order to make a comparison between the gene expression profile of the recurrent ameloblastoma sample and the other four samples, a separate analysis of samples 2, 3, 4 and 5 was also performed. It showed a total of 91 up-regulated genes and 110 down-regulated genes, at a multiple of 2-fold. The different number of up and down-regulated genes obtained using Benjamini and Hochberg false discovery rate filter as well as SAM is summarized in table 3. Among the 110 down-regulated genes *RAB31*, member of the RAS oncogene family was noted as well as Interleukin 17 receptor; adrenergic, beta, receptor kinase 2 and suppression of tumorigenicity 13 (colon carcinoma).

Table 1. LCM samples and aRNA quality assessment. Ameloblastoma tissue sections (7 µm) were stained with hematoxylin and eosin before performing LCM. The tissue prior to LCM (column 2), and the isolated tissue wedge after LCM (column 3),) is shown. For each sample, LCM was performed and the procured cells were pooled and RNA extracted and isolated. Column 4 shows the quality assessment graphs generated by the electrophoresis bioanalyzer, after each sample's aRNA was amplified
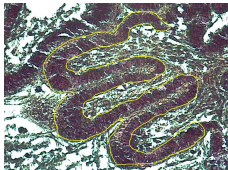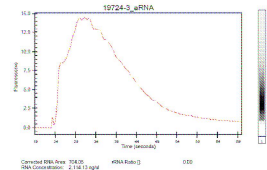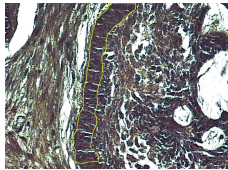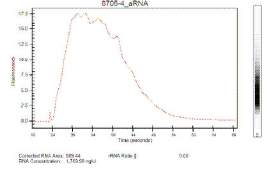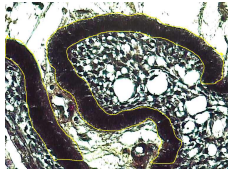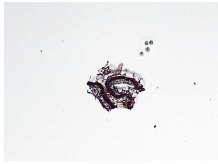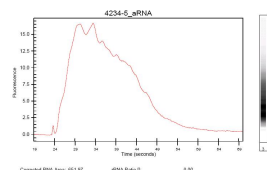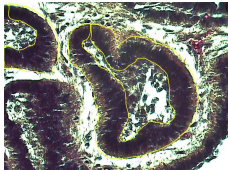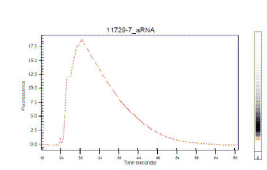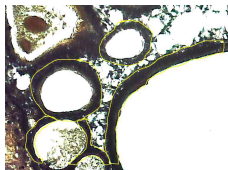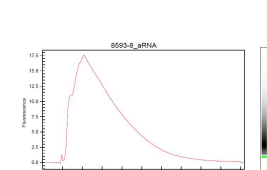
Sample	Before LCM	LCM	aRNA
Sample No.1 51 year old Female Recurrent ameloblastoma. Left posterior mandible			
Sample No. 2 27 year old female; left anterior mandible			
Sample No. 3 14 year old Female posterior right mandible			
Sample No. 4 34 year old Female Left posterior maxilla			
Sample No.5 17 years old Male Right posterior mandible			

Figure 1. Hierarchical clustering of the 5 arrays, 2 fold up and down-regulated genes; samples 4 and 5 share common gene expression; samples 2 and 3 have similar expression between them. Sample 1 is different and the closest to the human uRNA reference (It may represent a different gene expression in a recurrent ameloblastoma)

Table 2. Two-fold up-regulated genes present in all 5 ameloblastoma samples

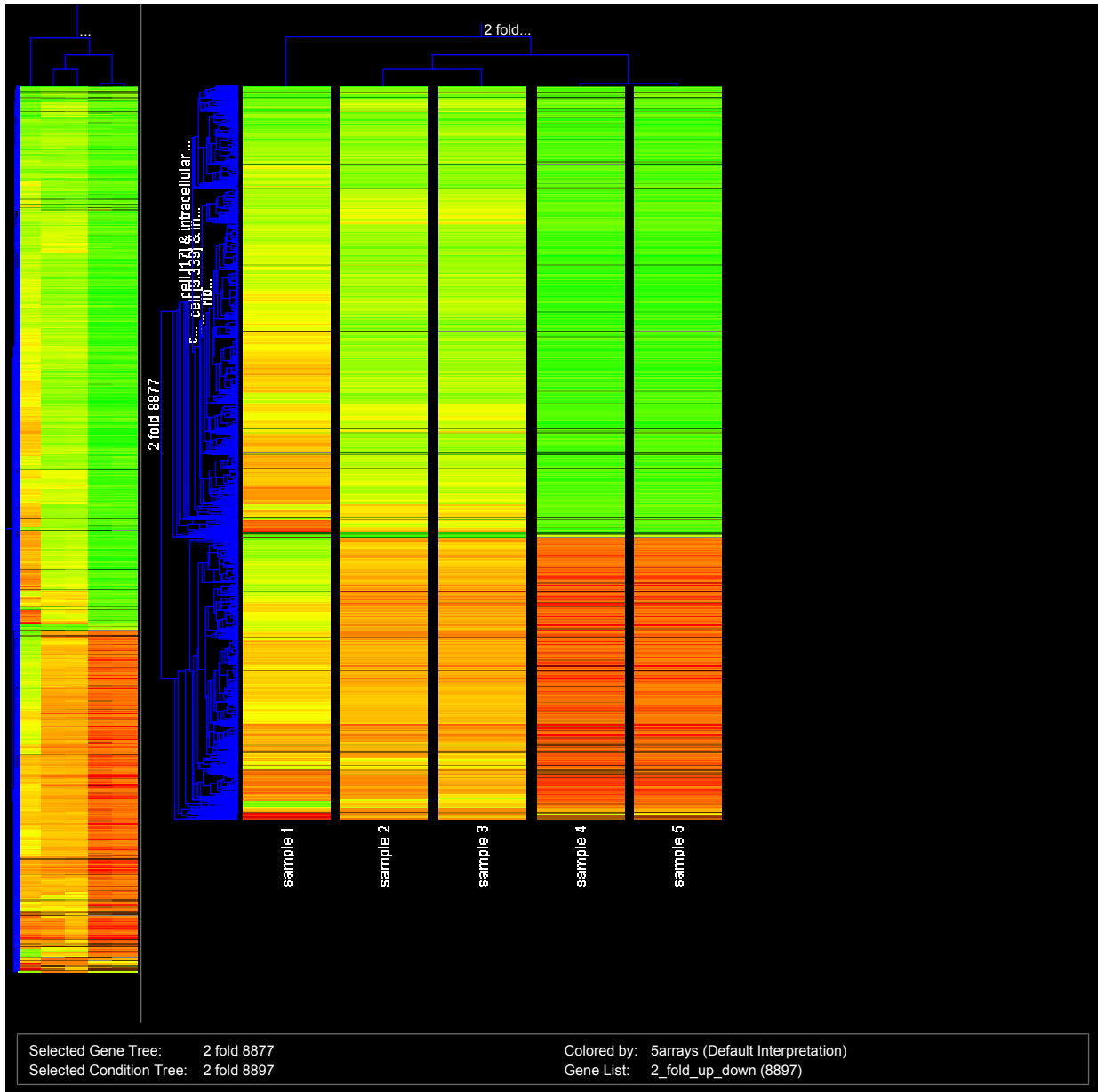| Common name	Biological process*	Molecular function*	Pathways
RAS-like, family 10, member B	small GTPase mediated signal transduction	GTP binding	
chromosome 21 open reading frame 70			
melanoma antigen family E, 1	GO:4(biological process unknown)	GO:5515(protein binding)	
MyoD family inhibitor	cell differentiation; cytoplasmic sequestering of transcription factor; embryonic development	receptor activity	
splicing factor, arginine/serine-rich 16 (suppressor-of-white-apricot homolog, Drosophila)	nuclear mRNA splicing, via spliceosome		
wingless-type MMTV integration site family, member 10A	development; frizzled-2 signaling pathway	signal transducer activity	KEGG pathway: Hedgehog signaling pathway 04340; KEGG pathway: Wnt signaling pathway 04310
acid phosphatase 5, tartrate resistant		acid phosphatase activity; hydrolase activity	KEGG pathway: Riboflavin metabolism 00740; KEGG pathway: gamma-Hexachlorocyclohexane degradation 00361
BTAF1 RNA polymerase II, B-TFIID transcription	negative regulation of transcription	ATP binding; helicase activity; transcription factor activity	
MYC binding protein 2	protein ubiquitination	ubiquitin-protein ligase activity; zinc ion binding	
sema domain, transmembrane domain (TM), and cytoplasmic domain, (semaphorin) 6A	apoptosis; axon guidance; cell surface receptor linked signal transduction; cytoskeleton organization and biogenesis; development; neurogenesis	protein binding; receptor activity	KEGG pathway: Axon guidance 04360
similar to zinc finger protein		nucleic acid binding; zinc ion binding	
zinc finger protein 265	RNA splicing	RNA binding; transcription factor activity	
leucine-rich repeat-containing G protein-coupled receptor 4	G-protein coupled receptor protein signaling pathway	protein-hormone receptor activity	
tenascin XB	cell-matrix adhesion	protein binding	KEGG pathway: ECM-receptor interaction 04512; KEGG pathway: Focal adhesion 04510

Common name	Biological process*	Molecular function*	Pathways
symplekin	cell adhesion	protein binding	KEGG pathway: Tight junction 04530
colipase, pancreatic	digestion; lipid catabolism	enzyme activator activity	
casein alpha s2-like A	transport	transporter activity	
dual specificity phosphatase 9	JNK cascade; inactivation of MAPK; protein amino acid dephosphorylation	MAP kinase phosphatase activity; hydrolase activity	KEGG pathway: MAPK signaling pathway 04010
UDP-N-acetyl-alpha-D-galactosamine:polypeptide N-acetylgalactosaminyltransf e*Rase* 10 (GalNAc-T10)		manganese ion binding; polypeptide N-acetylgalactosaminyltransfe*Rase* activity; sugar binding; transfe*Rase* activity, transferring glycosyl groups	KEGG pathway: O-Glycan biosynthesis 00512
zinc finger, CW type with coiled-coil domain 3		ATP binding	
OTU domain, ubiquitin aldehyde binding 1	GO:6955(immune response); GO:6512(ubiquitin cycle)	GO:8234(cysteine-type peptidase activity)	KEGG pathway: Biotin metabolism 00780; KEGG pathway: Lysine degradation 00310

*Gene Ontology

Table 3. Benjamini and Hochberg FDR and SAM. Number of genes 2 fold over-expressed in 5/5 samples and in 4/4 samples (after removing sample #1)

Samples	Multiple	Benjamini and Hochberg FDR $P < 0.05$	SAM
5/5	2-fold up	38	10
5/5	2-fold down	0	41
4/4	2-fold up	255	91
4/4	2-fold down	0	110

DISCUSSION

Using a microgenomics approach we have identified multiple molecular pathways that are likely to be involved in tumorigenesis and development of odontogenic tumors.

The oncogenes that were found to be involved in tumorigenesis and/or cell differentiation of ameloblastoma include *Ras (RAB31), c-Myc* and c*Fos* which corroborate the work of Heikinheimo et. al. who reported over-expression of the *Fos* oncogene (Heikinheimo,K. 2002). *RAB31*, a member of the *RAS* oncogene family, plays a role in GTPase mediated signal transduction and has a molecular function in GTP binding. It has been suggested that these oncogenes play a role in tumorigenesis via deregulation of cell proliferation.

DNA-repair genes are important during DNA replication. Polymerase (DNA directed), *gamma 2* was up-regulated in ameloblastomas. This gene product participates in ATP binding, single-stranded DNA binding and zinc ion binding as part of the DNA polymerase pathway.

There are several tumor-suppressor genes identified in the literature that are beleived to play a role in odontogenic tumors: retinoblastoma (RB), *p53*, adenomatous polyposis coli (*APC*), *WNT-1*, and patched (*PTC*) genes are well known (Ohki,K. 2004;144 Kumamoto,H. 2005). In this study, wingless-type MMTV integration site family, member 10A (*WNT10A*) proto-oncogene was found to be significantly up-regulated in ameloblastoma. *WNT10A* has a similar function to *WNT10B* in oncogenesis and in several developmental processes including regulation of cell fate and patterning during embryogenesis. It plays a key role in

carcinogenesis through activation of WNT-beta-catenin-TCF signaling pathway. As a ligand for members of the frizzled family of seven transmembrane receptors, it participates in signal transduction activity as part of the Hedgehog signaling pathway (KEGG pathway 04340) and the Wnt signaling pathway (KEGG pathway 04310). These gene products have been suggested as regulators of tooth development (Zhang, B. 2006). Gene products involved in cell growth that were found to be up-regulated in this study in ameloblastoma include T-cell acute lymphocytic leukemia 1; suppression of tumorigenicity 13 (colon carcinoma) as well as Fibroblast growth factor 13. The latter gene participates in cell-cell signaling, neurogenesis and signal transduction as part of MAPK signaling pathway and regulation of actin cytoskeleton pathway.

There are several categories of gene products identified with tumor progression. Among the cell-matrix adhesion molecules, integrin and alpha V (vitronectin receptor, alpha polypeptide, antigen CD51), which are part of the ECM-receptor interaction pathway, were over-expressed in ameloblastoma in this study. In the category of matrix-degrading proteinases, an over-expression of *MMP-1*, *MMP-2* and *MMP-9* was evident; these products are known to degrade basement membrane components contributing to local tumor invasion. Spondin 2, an extracellular matrix protein involved in cell adhesion, development, immune response and protein binding was also up-regulated.

Several signal transducers were down-regulated in the study samples, including ameloblastoma. Adrenergic, beta, receptor kinase 2, has molecular functions in ATP binding as well as G-protein coupled receptor kinase activity and

transferase activity. Interleukin 17 receptor is part of the cytokine-cytokine receptor interaction pathway; a gene product labeled "similar to Laminin receptor 1", a structural constituent of ribosome was also down-regulated in ameloblastoma possibly affecting the receptor activity. A partial list of the most relevant up-regulated and down-regulated genes is presented in Table 4. This analysis is just the beginning of many future studies to continue the evaluation of the possible role of many other genes in the tumorigenesis of ameloblastoma. Perhaps there is a gene that can be manipulated chemically in order to reduce the size of the tumor and to prevent high morbidity which will benefit those patients who do not have readily available access to health care.

Table 4. Summary of gene products implicated in tumorigenesis and progression in ameloblastoma

TUMORIGENESIS	
Oncogenes	*Ras*, Myc, *Fos*,
Growth Factors	T-cell acute lymphocytic leukemia 1 Suppression of tumorigenicity 13 Fibroblast growth factor 13 (*FGF13*)
Tumor suppressor genes	Wingless-type MMTV 10A (*WNT-10A*)
TUMOR PROGRESSIONN	
cell-matrix adhesion molecules	Integrin, Spondin 2,
signal transducers	Beta, adrenergic, receptor kinase 2 Interleukin 17 Similar to Laminin receptor 1

CONCLUSION

This study is the first to report the results of combining laser capture micodissection and microarray gene expression profiling in formalin fixed decalcified paraffin embedded ameloblastoma. Studies such as this, using oligonucleotide array experiments from small sample aRNA specimens are likely to generate additional functionally important data in the future that reflects the biological differences among disease entities. Many of the genes that were over-expressed in the study are involved in the regulation of oncogenesis, cell adhesion and signal transduction. Ameloblastoma is an aggressive tumor with a significant recurrence rate and potentially devastating functional effects on the patient. Presently, surgery is the therapy of choice for most ameloblastomas. The results of this investigation are exiting in that they reveal the possibility of utilizing proteins and receptor-factors from gene expression profiles to enhance the results of surgery alone. This can result in substantially decreased morbidity for the patient.

APPENDIX

Table A1. Tissue scrapes Ameloblastoma samples: total RNA characterization

The lower 260/280 ratio (expected range 1.8 – 2.1) is due to degradation of RNA after formalin fixation of the tissue. The reverse transcription equivalent score (RTE) was established to obtain total RNA input required into an amplification process. This score is determined by using the 3' beta-actin Ct (threshold cycle) value equivalent of 100pg human universal RNA (uRNA).

Sample ID	ng/ul	260/280	Total yield (ng)	3'/5' ratio	RTE score
19724-3	17.1	1.43	256.5	12.6	11.5 ng
6705-4	34.2	1.39	513	14	14 ng
4234-5	20.4	1.58	306	13.84	13 ng
11729-7	67.6	1.74	1014	15.9	11.2 ng
8593-8	31.5	1.49	472.5	13.69	17 ng

Table A2. Laser capture microdissection (LCM). Characterization of the total RNA extracted from captured samples.

Sample ID	Total RNA characterization		
	ng/ul	260/280	Yield (ng)
19724-3	9.9	1.45	148.5
6705-4	29.7	1.64	445.5
4234-5	16	1.66	240
11729-7	36.4	1.52	546
8593-8	21.6	1.65	324

Table A3. RNA amplification. Total yield of aa-aRNA obtained from seven samples, including five LCM samples, positive control (uRNA) and a negative control (no template).

samples	RNA input	aa-aRNA characterization		
		ng/µl	260/280	Total yield (ng)
19724-3_aRNA	10 ng	1905.2	2.13	42867
6705-4_aRNA	10 ng	2115.9	2.12	47607.75
4234-5_aRNA	10 ng	2083.3	2.12	46874.25
11729-7_aRNA	10 ng	1746.4	2.14	39294
8593-8_aRNA	10 ng	1809.8	2.14	40720.5
Positive control	100 pg	1982.7	2.07	44610.75
Negative control	0 pg	31.8	1.88	715.5

Table A4. Comparison of hybridization signal intensities. **Blue** indicates the mean scaled hybridization intensity. **Read and green** are probe-sets that change more than twofold between the samples being compared. Each *y* axis is the log intensity of the single sample indicated. Each *x* axis is the log mean intensity of all samples.

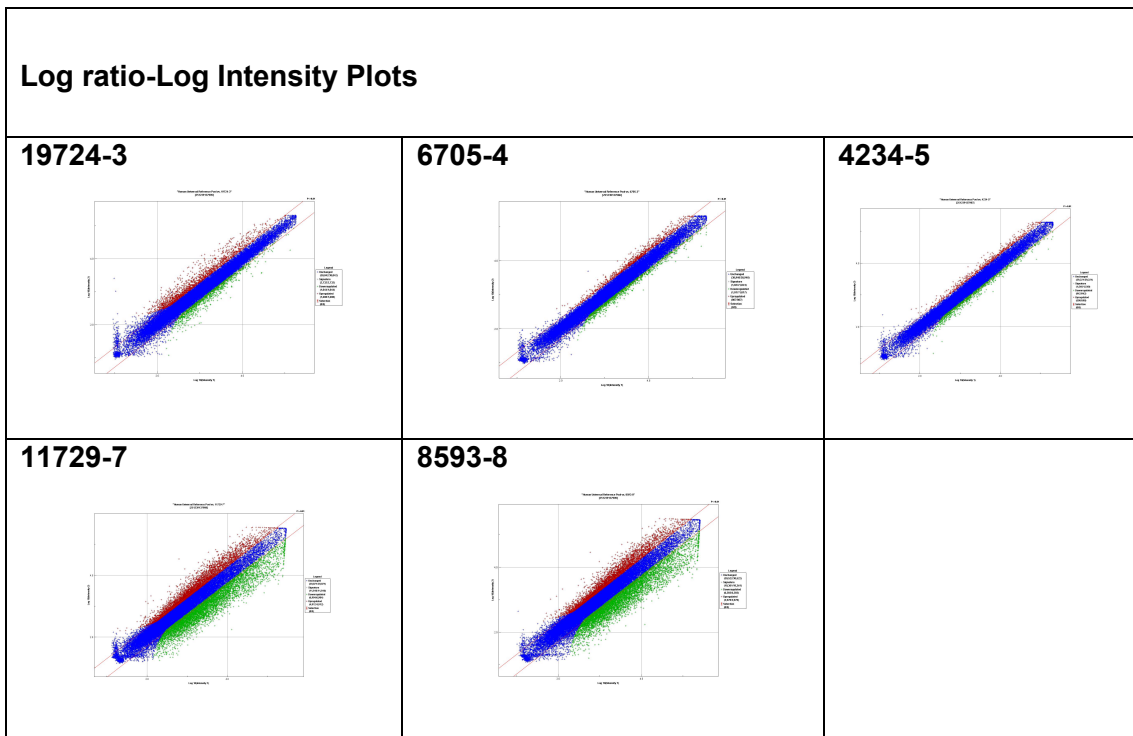| Log ratio-Log Intensity Plots		
19724-3 	**6705-4** 	**4234-5**
11729-7 	**8593-8** 	

Table A5. SAM analysis for a set of Delta (Δ). The false discovery rate (FDR) is defined as the percentage of falsely significant genes compared to the genes called significant.

SAM Analysis for a set of Delta (Δ)					
delta	p	0	Number falsely significant	Number called significant	FDR
1	0.2	0.433	24623.52	32095	0.332
2	0.4	0.433	12430.98	23207	0.232
3	0.6	0.433	3733.86	12295	0.131
4	0.8	0.433	1415.09	7780	0.079
5	1.0	0.433	669.04	5562	0.052
6	1.2	0.433	334.88	4255	0.034
7	1.4	0.433	189.63	3319	0.025
8	1.6	0.433	114.08	2632	0.019
9	1.8	0.433	76.92	2154	0.015
10	2.0	0.433	50.41	1726	0.013
11	2.2	0.433	32.52	1404	0.010
12	2.4	0.433	24.84	1186	0.009
13	2.6	0.433	19.14	1000	0.008
14	2.8	0.433	15.49	842	0.008
15	3.0	0.433	13.10	704	0.008

Figure A1 (A and B). Reverse Transcription - quantitative Polymerase **Chain Reaction (RT-qPCR): standard curve for 3'beta actin (A) and 5'beta actin (B).**

Real Time- PCR was used to measure the RNA quality and quantity from tissue scrapes. In addition to the RNA samples, a control RNA was run to serve as template for a standard curve enabling quantitation of the sample material. Two primer sets were designed for beta-actin mRNA. The ratio of the RNA quantity 3' and 5" beta-actin Ct (threshold cycle) is an indicator of the quality of RNA. Ratio value up to 10 indicates good RNA quality for microarray analyses and ratio value above 50 represent poorer quality RNA sample.
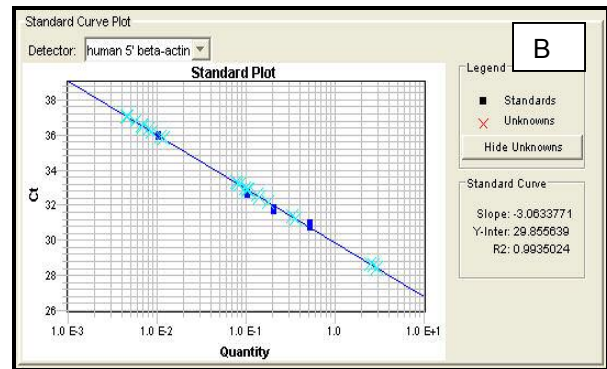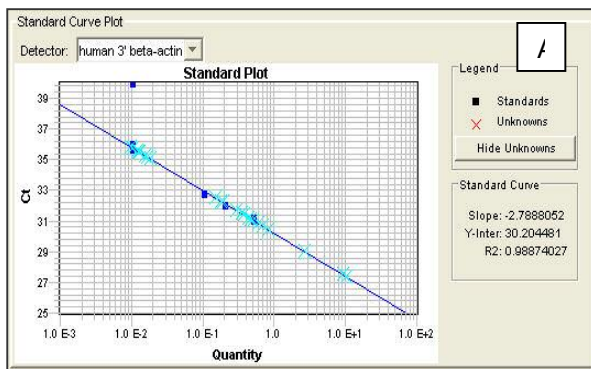
Figure A2. Identification of genes with significant changes in expression, using SAM. Scatter plot of the observed relative difference d(i) versus the expected relative difference d(i). The solid line indicates the line for observed d(i)=expected d(i), where the observed relative difference is identical to the expected relative difference. The dotted lines are drawn at a distance of $\Delta = 1.2$ from the solid line. The cutoffs for 2-fold induction and repression are indicated by the dashed lines. The potentially significant genes are indicated by the circles
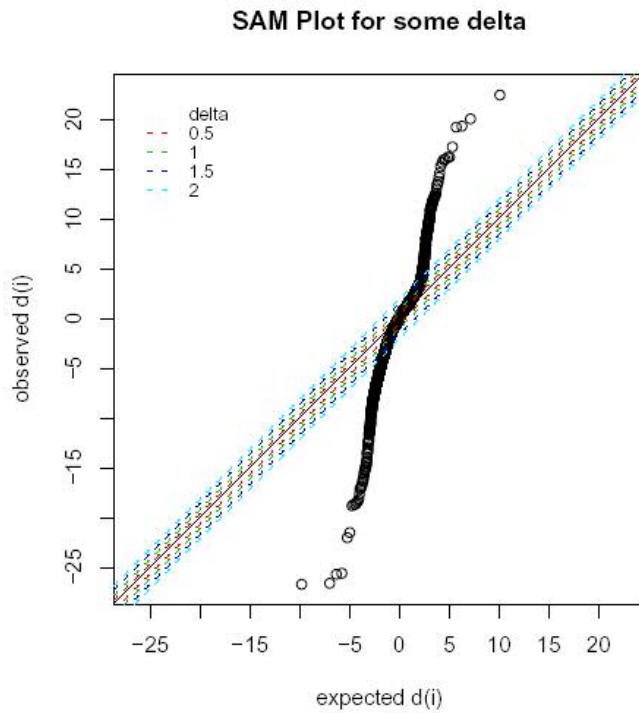
REFERENCES

Carinci F, Francioso F, Piattelli A, Rubini C, Fioroni M, Evangelisti R, Arcelli D, Tosi L, Pezzetti F, Carinci P, Volinia S. (2003). Genetic expression profiling of six odontogenic tumors. J. Dent. Research 2003 Jul;82(7):551-7.

Emmert-Buck, M. R., Bonner, R. F., Smith, P. D., Chuaqui, R. F., Zhuang, Z., & Goldstein, S. R. et al. (1996). Laser capture microdissection. *Science, 274*(5289), 998-1001.

Heikinheimo, K., Jee, K. J., Niini, T., Aalto, Y., Happonen, R. P., & Leivo, I. et al. (2002). Gene expression profiling of ameloblastoma and human tooth germ by means of a cDNA microarray. *Journal of Dental Research, 81*(8), 525-530.

Jaaskelainen, K., Jee, K. J., Leivo, I., Saloniemi, I., Knuutila, S., & Heikinheimo, K. (2002). Cell proliferation and chromosomal changes in human ameloblastoma. *Cancer Genetics and Cytogenetics, 136*(1), 31-37.

Keszler, A., Paparella, M. L., & Dominguez, F. V. (1996). DeSMOplastic and non-deSMOplastic ameloblastoma: A comparative clinicopathological analysis. *Oral Diseases, 2*(3), 228-231.

King, C., Guo, N., Frampton, G. M., Gerry, N. P., Lenburg, M. E., & Rosenberg, C. L. (2005). Reliability and reproducibility of gene expression measurements using amplified RNA from laser-microdissected primary breast tissue with oligonucleotide arrays. *Journal of Molecular Diagnostics : JMD, 7*(1), 57-64.

Kumamoto, H., & Ooya, K. (2005). Expression of tumor necrosis factor alpha, TNF-related apoptosis-inducing ligand, and their associated molecules in ameloblastomas. *Journal of Oral Pathology & Medicine : Official Publication of the International Association of Oral Pathologists and the American Academy of Oral Pathology, 34*(5), 287-294.

Kumamoto, H., Yoshida, M., & Ooya, K. (2001). Immunohistochemical detection of amelogenin and cytokeratin 19 in epithelial odontogenic tumors. *Oral Diseases, 7*(3), 171-176.

Larsson, O., Wahlestedt, C., & Timmons, J. A. (2005). Considerations when using the significance analysis of microarrays (SAM) algorithm. *BMC Bioinformatics [Computer File], 6*(1), 129.

Li, T. J., Wu, Y. T., Yu, S. F., & Yu, G. Y. (2000). Unicystic ameloblastoma: A clinicopathologic study of 33 chinese patients. *The American Journal of Surgical Pathology, 24*(10), 1385-1392.

Leethanakul, C., Knezevic, V., Patel, V., Amornphimoltham, P., Gillespie, J., & Shillitoe, E. J. et al. (2003). Gene discovery in oral squamous cell carcinoma through the head and neck cancer genome anatomy project: Confirmation by microarray analysis. *Oral Oncology, 39*(3), 248-258.

Luo, L., Salunga, R. C., Guo, H., Bittner, A., Joy, K. C., & Galindo, J. E. et al. (1999). Gene expression profiles of laser-captured adjacent neuronal subtypes. *Nature Medicine, 5*(1), 117-122.

Luzzi, V., Holtschlag, V., & Watson, M. A. (2001). Expression profiling of ductal carcinoma in situ by laser capture microdissection and high-density oligonucleotide arrays. *American Journal of Pathology, 158*(6), 2005-2010.

Luzzi, V., Mahadevappa, M., Raja, R., Warrington, J. A., & Watson, M. A. (2003). Accurate and reproducible gene expression profiles from laser capture microdissection, transcript amplification, and high density oligonucleotide microarray analysis. *Journal of Molecular Diagnostics : JMD, 5*(1), 9-14.

Naderi, A., Ahmed, A. A., Barbosa-Morais, N. L., Aparicio, S., Brenton, J. D., & Caldas, C. (2004). Expression microarray reproducibility is improved by optimising purification steps in RNA amplification and labelling. *BMC Genomics [Computer File], 5*(1), 9.

Nodit, L., Barnes, L., Childers, E., Finkelstein, S., Swalsky, P., & Hunt, J. (2004). Allelic loss of tumor suppressor genes in ameloblastic tumors. *Modern Pathology : An Official Journal of the United States and Canadian Academy of Pathology, Inc, 17*(9), 1062-1067.

Novoradovskaya, N., Whitfield, M. L., Basehore, L. S., Novoradovsky, A., Pesich, R., & Usary, J. et al. (2004a). Universal reference RNA as a standard for microarray experiments. *BMC Genomics [Computer File], 5*(1), 20.

Novoradovskaya, N., Whitfield, M. L., Basehore, L. S., Novoradovsky, A., Pesich, R., & Usary, J. et al. (2004b). Universal reference RNA as a standard for microarray experiments. *BMC Genomics [Computer File], 5*(1), 20.

Ohyama, H., Mahadevappa, M., Luukkaa, H., Todd, R., Warrington, J. A., & Wong, D. T. (2002). Use of laser capture microdissection-generated targets for hybridization of high-density oligonucleotide arrays. *Methods in Enzymology, 356*, 323-333.

Ohyama, H., Zhang, X., Kohno, Y., Alevizos, I., Posner, M., & Wong, D. T. et al. (2000). Laser capture microdissection-generated target sample for high-density oligonucleotide array hybridization. *BioTechniques, 29*(3), 530-536.

Schena, M., Shalon, D., Davis, R. W., & Brown, P. O. (1995). Quantitative monitoring of gene expression patterns with a complementary DNA microarray. *Science, 270*(5235), 467-470.

Shibata, D., Hawes, D., Li, Z. H., Hernandez, A. M., Spruck, C. H., & Nichols, P. W. (1992). Specific genetic analysis of microscopic tissue after selective ultraviolet radiation fractionation and the polymerase chain reaction. *American Journal of Pathology, 141*(3), 539-543.

Taylor, T. B., Nambiar, P. R., Raja, R., Cheung, E., Rosenberg, D. W., & Anderegg, B. (2004). Microgenomics: Identification of new expression profiles via small and single-cell sample analyses. *Cytometry A., 59*(2), 254-261.

Tusher, V. G., Tibshirani, R., & Chu, G. (2001). Significance analysis of microarrays applied to the ionizing radiation response. *Proceedings of the National Academy of Sciences of the United States of America, 98*(9), 5116-5121.

Van Gelder, R. N., von Zastrow, M. E., Yool, A., Dement, W. C., Barchas, J. D., & Eberwine, J. H. (1990). Amplified RNA synthesized from limited quantities of heterogeneous cDNA. *Proceedings of the National Academy of Sciences of the United States of America, 87*(5), 1663-1667.

Vickers, R. A., & Gorlin, R. J. (1970). Ameloblastoma: Delineation of early histopathologic features of neoplasia. *Cancer, 26*(3), 699-710.

Waldron, C. A. (1966). Ameloblastoma in perspective. *Journal of Oral Surgery (American Dental Association : 1965), 24*(4), 331-333.

Waldron, C. A., & el-Mofty, S. K. (1987a). A histopathologic study of 116 ameloblastomas with special reference to the deSMOplastic variant. *Oral Surgery, Oral Medicine, and Oral Pathology, 63*(4), 441-451.

Waldron, C. A., & el-Mofty, S. K. (1987b). A histopathologic study of 116 ameloblastomas with special reference to the deSMOplastic variant. *Oral Surgery, Oral Medicine, and Oral Pathology, 63*(4), 441-451

Webb, T. (2000). Laser capture microdissection comes into mainstream use. *Journal of the National Cancer Institute, 92*(21), 1710-1711.

Zhang, L., Zhou, W., Velculescu, V. E., Kern, S. E., Hruban, R. H., & Hamilton, S. R. et al. (1997). Gene expression profiles in normal and cancer cells. *Science, 276*(5316), 1268-1272.